Journal of Applied Fluid Mechanics, Vol. 9, No. 3, pp. 1265-1272, 2016.
Available online at www.jafmonline.net, ISSN 1735-3572, EISSN 1735-3645.
DOI: 10.18869/acadpub.jafm.68.228.22982

Effect of Rotation on Natural Convection in Differentially Heated Rotating Enclosure by Numerical Simulation

M. Narendra Kumar[1] G. Pundarika[2] K. Rama Narasimha[3†] and K. N. Seetharamu[4]

[1,3] *Centre for Emerging Technologies, Jain University, Bangalore, Karnataka, 562112, India*
[2] *Government Engineering College, Ramanagara, Karnataka, 571511, India*
[4] *PES University, Bangalore,Karnataka, 560085, India*

†*Corresponding Author Email:k.ramanarasimha@gmail.com*

(Received May 6, 2014; accepted June 24, 2015)

ABSTRACT

Natural convection heat transfer in a two dimensional unsteady rotating differentially heated enclosure is studied numerically in this paper. The enclosure is filled with air and executes a steady counterclockwise rotation about the centre of the enclosure. A finite volume code on a staggered grid arrangement with TDMA algorithm is developed and employed to solve the governing equations subject to Boussinesq approximation. The numerical investigation is carried out for fixed Prandtl number equal to 0.71, Rayleigh number equal to1.1×10^5 while Taylors number vary from5.2×10^4 to $3.3 \times 10^5$and Rotational Rayleigh number from 4.9×10^2 to 3.1×10^3.Results reveal that there are considerable change in heat transfer rates beyond 15 rpm. The effect of rotation on the Nusselt number for a given Rayleigh number is shown in the present work which is not normally indicated and discussed in the available literature

Key words: Rotating enclosure; Natural convection; Coriolis force; Heat transfer.

NOMENCLATURE

k	thermal conductivity (W/m-K)
L	length of the enclosure (m)
Nu	local Nusselt number
P	dimensionless pressure
p,Pm	pressure and motion pressure (N/m^2)
Pr	Prandtl number
Ra	Rayleigh Number
Ra_w	rotational Rayleigh number system
T	temperature (K)
t	time (s)
Ta	taylor number
u, v	dimensional velocity components (m/s)
U, V	dimensionless velocity components
X, Y	dimensionless Cartesian coordinate
x,y	dimensional Cartesian coordinate system
Ω	magnitude of angular rotation rate (rpm, rad/s)
α	thermal diffusivity (m^2/s)
τ	dimensionless time
θ	dimensionless temperature
ϕ	angular position of enclosure (^{o})
ρ	density (kg/m^3)
μ	dynamic viscosity (Pas)

Subscript

c	cold
h	hot
f	fluid

Superscript

-	space average
=	Time average

1. INTRODUCTION

The fluid flow and heat transfer characteristics of a rotating enclosure were treated in detail according to its functional and practical importance in the thermal management. The unsteady rotating conditions are encountered in situations such as rotary machines, guided missiles and space-based manufacturing processes. Bobco (1981) introduced the application of natural convection in the design of a vented Gallileo mission descent module parachuting into the Jupiter atmosphere. It was reported by Yeh (1995) that the failure caused by

temperature and vibration amounts to 75% of all failures. There had been many studies on flow in rotating ducts, for instance in relation to cooling of turbine blades by Lin *et al.* (2001). Rossby (1969) experimentally observed the subcritical instability in a water layer for $Ta > 5 \times 10^4$ and in an air layer for $Ta < 10^5$. In addition, for water at $Ra > 10^4$,the Nusselt number was found to increase with the Taylor number. The opposite trend is the case for air. Besides, at a large Taylor number, oscillatory convection is preferred in mercury. Buhler and Oertel (1982) studied the thermal cellular convection in a rotating rectangular box filled with a viscous fluid and found that the roll cells changed orientation with increasing Taylor number. The flow and heat transfer characteristics of a rotating square enclosure are studied experimentally and numerically by Hamady *et al*. (1994). They concluded that the Coriolis force arising from rotation may have a remarkable influence on heat transfer when compared to non rotating results. Ker and Lin (1996, 1997) studied a differential heated rotating cubic enclosure. Significant flow modifications are obtained when the rotational Rayleigh number is greater than the Rayleigh number. A significant increase or decrease in heat transfer could be achieved due to rotation as reported by Baig *et al*.(2001, 2006). Jin *et al*.(2005)carried out numerical studies on a rectangular enclosure with discrete heat source. They found that rotation results in an imbalance between clockwise and counter-clockwise circulations, increases heat transfer and reduces the oscillations of Nusselt number. It improves or reduces the average performance in each cycle. The effects of Coriolis force, centrifugal force and thermal buoyancy force are segregated numerically on a differentially heated square enclosure by Tso *et al*.(2007)

However, there are limited studies on unsteady natural convection cooling from differentially heated sources in rotation. The situation with natural convection is very different from forced convection because the latter is pressure-driven flow where as the centrifugal force plays an important role and the thermal buoyancy effect is neglected. In a sense, there is no absolute stationary state on earth, since Taylor number, normally used to reflect the effect of Coriolis force in the rotating fluid, is about unity at the equatorial sea level. (Boubnov and Golitsyn 1995).

A detailed 3-D numerical computation for this differentially heated source condition is formidable, especially with the influence of the buoyancy force, Coriolis force and centrifugal force all within the same frame. When the enclosure is rotated, it is still challenging and useful to study a 2-D model as reported by Jin *et al*. (2005).

In the present work, it is intended to study the effects of rotation on natural convection in a square enclosure, with differentially heated top and bottom walls. The effect of rotational speeds on the characteristics of fluid flow as well heat transfer rate are considered.

2. MATHEMATICAL FORMULATION

The schematic diagram of the physical system under investigation is depicted in Fig.1. Initially at time$t \leq 0$, the enclosure and inside air are both stationary and isothermal atT_o. At $t > 0$,the enclosure executes a steady uniform counter clockwise rotation about a horizontal axis. The surface at$y = L/2$is subjected to uniform temperature T_h and the surface at $y = -L/2$, subjected to uniform temperatureT_c. The lateral walls are thermally well insulated from the surroundings. The ϕ in Fig. 1 defines the angular position of the enclosure. Thus the air flow inside the enclosure is simultaneously driven by the rotation and the thermal buoyancies. By adopting the Boussinesq approximation, (Buhler and Oertel 1982; Ker and Lee 1996 and Jin *et al*. 2005) linear density variation with temperature is considered in both the body force and centrifugal force terms. The terms representing the thermal and rotational buoyancies and Coriolis force are, respectively, equal to $\rho_o \vec{g}\beta(T - T_c), -\rho_o \vec{g}\beta(T - T_c)\vec{\Omega} \times (\vec{\Omega} \times \vec{r}$ and$-2\rho_o[1 - \beta(T - T_c)]\Omega \times V$. The resulting flow development can be described as follows:

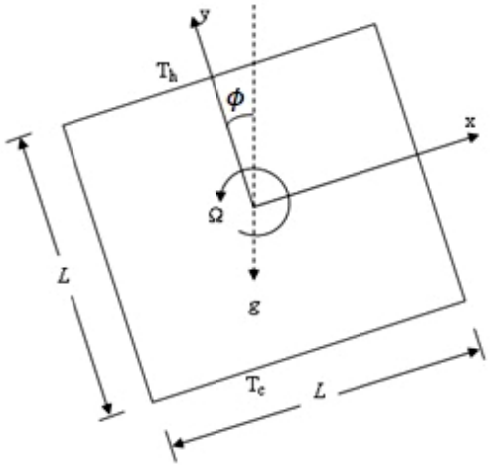

Fig. 1. Schematic representation of the physical system.

The continuity, momentum and energy equations are

$$\frac{\partial u}{\partial x} + \frac{\partial v}{\partial y} = 0 \tag{1}$$

$$\frac{\partial u}{\partial t} + u\frac{\partial u}{\partial x} + v\frac{\partial u}{\partial y} = -\frac{1}{\rho_o}\frac{\partial p}{\partial x} + \upsilon\left[\frac{\partial^2 u}{\partial x^2} + \frac{\partial^2 u}{\partial y^2}\right] + g\beta(T - T_c)\sin(\Omega t) - \beta(T - T_c)\Omega \times (\Omega x) - 2\Omega v + 2\beta(T - T_c)\Omega v \tag{2}$$

$$\frac{\partial v}{\partial t} + u\frac{\partial v}{\partial x} + v\frac{\partial v}{\partial y} = -\frac{1}{\rho_o}\frac{\partial p}{\partial y} + \upsilon\left[\frac{\partial^2 v}{\partial x^2} + \frac{\partial^2 v}{\partial y^2}\right] + g\beta(T - T_c)\cos(\Omega t) - \beta(T - T_c)\Omega \times (\Omega y) + 2\Omega u + 2\beta(T - T_c)\Omega u \tag{3}$$

$$\frac{\partial T}{\partial t}+u\frac{\partial T}{\partial x}+v\frac{\partial T}{\partial y}=\alpha\left(\frac{\partial^2 T}{\partial x^2}+\frac{\partial^2 T}{\partial y^2}\right) \tag{4}$$

Boundary Conditions are

$$\left.\begin{aligned} &At\ \ x=-\frac{L}{2},\ u=v=0,\ \frac{\partial T}{\partial x}=0\\ &At\ x=\frac{L}{2},\ u=v=0,\ \frac{\partial T}{\partial x}=0\\ &At\ y=-\frac{L}{2},\ u=v=0,\ T=T_c\\ &At\ y=\frac{L}{2},\ u=v=0,,\ \ T=T_h \end{aligned}\right\} \tag{5}$$

With the motion pressure defined as

$$P_m=\left[-\frac{1}{2}\Omega^2x^2-\frac{1}{2}\Omega^2y^2+gx\sin(\Omega t)+gy\cos(\Omega t)\right] \tag{6}$$

As mentioned by Vanyo (1993) in a rotating Eulerian coordinate system the centrifugal term can be included in the pressure term and disappears from the typical rotating fluid computation. With Boussinesq approximation, the main part of the centrifugal force term is combined with the pressure term and others are caused by density change and centrifugal buoyancy. The governing equations can be converted to non-dimensional forms using the non-dimensional parameters as indicated in (7).

$$\left.\begin{aligned} &X=\frac{x}{L}\ Y=\frac{y}{L}\ U=\frac{uL}{\alpha}\ V=\frac{vL}{\alpha}\ \ \tau=\frac{t\alpha}{L^2}\ P=\frac{P_mL^2}{\rho\alpha^2}\\ &\theta=\left(\frac{T-T_c}{T_h-T_c}\right)\quad \Pr=\frac{\nu}{\alpha}\quad Ra=\frac{g\beta(T_h-T_c)L^3}{\nu\alpha}\\ &Ra_w=\frac{\beta\Omega^2(T_h-T_c)L^4}{\nu\alpha}\ \ Ta=\frac{4\Omega^2L^4}{\nu^2} \end{aligned}\right\} \tag{7}$$

The Coriolis buoyancy force is neglected as $|\beta(T-T_c)|\ll 1$in the present study [Jin *et al.* (2005)]. The dimensionless governing equations and boundary conditions are written as follows:-

Continuity equation:

$$\frac{\partial U}{\partial X}+\frac{\partial V}{\partial Y}=0 \tag{8}$$

Momentum equations:

$$\begin{aligned} &\frac{\partial U}{\partial \tau}+U\frac{\partial U}{\partial X}+V\frac{\partial U}{\partial Y}=-\frac{\partial P}{\partial X}+Pr\left(\frac{\partial^2 U}{\partial X^2}+\frac{\partial^2 U}{\partial Y^2}\right)\\ &\quad+\left(Ta^{0.5}\Pr V\right)-\left(Ra_wPr\theta X\right)\\ &\quad+\left(RaPr\theta\right)\sin\left(0.5Ta^{0.5}Pr\tau\right) \end{aligned} \tag{9}$$

$$\begin{aligned} &\frac{\partial V}{\partial \tau}+U\frac{\partial V}{\partial X}+V\frac{\partial V}{\partial Y}=-\frac{\partial P}{\partial Y}+Pr\left(\frac{\partial^2 V}{\partial X^2}+\frac{\partial^2 V}{\partial Y^2}\right)\\ &\quad-\left(Ta^{0.5}\Pr U\right)-\left(Ra_wPr\theta X\right)\\ &\quad+\left(RaPr\theta\right)\cos\left(0.5Ta^{0.5}Pr\tau\right) \end{aligned} \tag{10}$$

Energy equation:

$$\frac{\partial \theta}{\partial \tau}+U\frac{\partial \theta}{\partial X}+V\frac{\partial \theta}{\partial Y}=\frac{\partial^2 \theta}{\partial X^2}+\frac{\partial^2 \theta}{\partial Y^2} \tag{11}$$

Boundary Conditions:

$$\left.\begin{aligned} &At\ \ X=-0.5,\ U=V=0,\ \frac{\partial\theta}{\partial X}=0\\ &At\ X=0.5,\ U=V=0,\ \frac{\partial\theta}{\partial X}=0\\ &At\ Y=-0.5,\ U=V=0,\ \theta=-0.5\\ &At\ Y=0.5,\ U=V=0,\quad \theta=0.5 \end{aligned}\right\} \tag{12}$$

The above formulation clearly shows that the flow to be examined is governed by dimensionless parameters, namely Prandtl number, Rayleigh number and Taylor number and rotational Rayleigh number. The rotational Rayleigh number reflects the effect of the rotational buoyancy force which depends on the other non-dimensional parameters. The rotational buoyancy becomes important when the rotational speed is high or the enclosure dimensions are too large, viz is whenΩ^2L is much larger than g (Lin *et al*. 1996).

The fluid motion is displayed using the stream function obtained from the velocity components U and $V$and the temperature fields using the isotherms. In addition to the time evaluation of velocity and temperature fields, results for the local, spaced averaged and time space averaged Nusselt number (Nu)on the heated or cooled wall are important in thermal design and can be evaluated from

$$\left.\begin{aligned} &Nu=\left.\frac{\partial\theta}{\partial Y}\right|_{Y=\pm0.5}\\ &\overline{Nu}=\int_{-0.5}^{0.5}NudX\\ &\overline{\overline{Nu}}=\frac{1}{2\pi n}\int_0^{2\pi n}\overline{Nu}d\varphi \end{aligned}\right\} \tag{13}$$

3. SOLUTION METHODOLOGY

For this unsteady problem, a finite volume code is developed using the SIMPLE Scheme as explained by Patankar (1980) for coupling pressure and velocity on staggered grid arrangement. The TDM Aalgorithm is adopted to solve the governing equations (8-11) subjected to the boundary conditions (12). Due to the lack of pressure boundary conditions, the use of staggered grid arrangement provides an advantage. That is one may locate the secondary grid along the boundaries of the domain where the specification of velocity boundary conditions is required but not the pressure. An upwind difference scheme is used for the convective terms because of its simplicity and improved stability properties. The central difference scheme is used for the diffusion terms and a first order implicit scheme is used for the unsteady term. The discretized governing equations are solved iteratively through a line-by-

line application of the TDMA algorithm, enforcing under-relaxation to ensure convergence at each time step considered. In the iteration procedure, the motion pressure correction equations are used to derive the new velocity from the previous calculated velocity. To check the convergence of the sequential iterative solution, the sum of the absolute differences of the solution variables between two successive iterations has been evaluated. When this summation falls below the convergence criterion, convergence is obtained. The convergence criterion has been chosen as 10^{-5}in this study. A dedicated Fortran Code based on Finite Volume Method is developed indigenously to solve the natural convection problem in enclosure with rotation.

4. RESULTS AND DISCUSSION

The analysis in the present numerical investigation is performed in the following dimensionless groups: $Pr = 0.71,\quad Ra = 1.1 \times 10^5,\quad Ta = 5.2 \times 10^4\ to\ 3.3 \times 10^5$, and $Ra_w = 4.9 \times 10^2\ to\ 3.1 \times 10^3$. $Ra_w$is not discussed except to specify it explicitly. This is due to the Ra_w not being an independent parameter but depending on Pr and Raas well as on Ta. Other parameter is$\Omega = 10rpm\ to\ 25\ rpm$

4.1 Grid Testing and Code Validation

Uniform grid distribution is used for the whole enclosure. The effect of grid resolution was examined in order to select the appropriate grid density. Appropriate grid densities among a range from $31 \times 31\ to\ 81 \times 81$are considered to study grid independence. After 61×61 grids, there is no considerable change in the average Nusselt number. Considering the accuracy required and the computational time involved, a 61×61 grid is chosen for the present study as exhibited in Fig. 2.

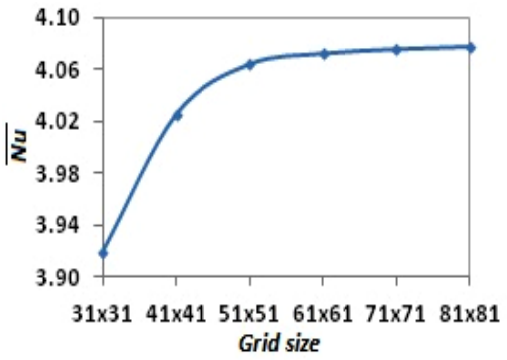

Fig. 2. Grid independency study $\overline{Nu}$ versus grid size for$Pr = 0.71,\ Ra = 1.1 \times 10^5\ and\ \Omega = 10\ rpm$.

As a validation, the present results of the code for the isotherms compare well with that obtained by Hamady *et al.* (1994) and with. Jin *et al.*(2005) as shown in Fig. 3.

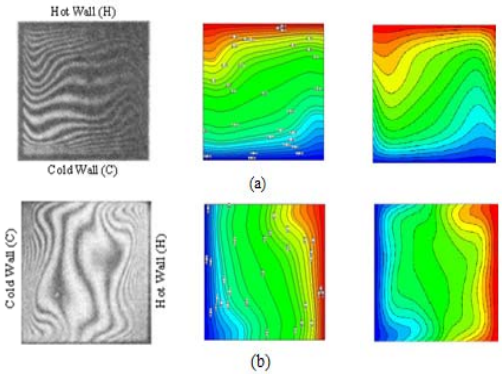

Fig. 3. Comprasion of computed Isotherms of present work (middle) with Hamady et al. (left) and with Jin et al. (right) (a) $\phi = 0°$, (b) $\phi = 270°, Pr = 0.71,\ Ra = 1.1 \times 10^5\ and\ \Omega = 15\ rpm$.

Fig. 4. (a) and (b) shows the half sectioned isotherms of the present work matched with that of the experimental work of Hamady et al. (1994) for the two angular position of the enclosure considered with$\phi = 0°$ and $\phi = 270°$. The isotherms of the present case very closely match with that of the experimental work.

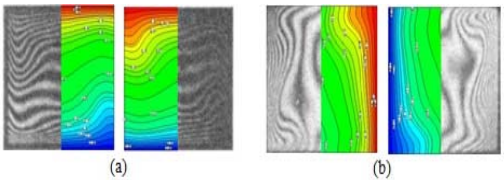

Fig. 4. Comprasion of computed Isotherms of present work with Hamady et al.(a) $\phi = 0°$ (b) $\phi = 270°, Pr = 0.71,\ Ra = 1.1 \times 10^5\ and\ \Omega = 15\ rpm$.

Fig. 5 and 6 show the variation of the computed dimensionless temperature along dimensionless length of the enclosure of the present work at two different positions of the enclosureand comparedwith that of Hamady *et al.* (1994). These figures show good agreement of the present work with the experimental work of Hamady *et al.* (1994).

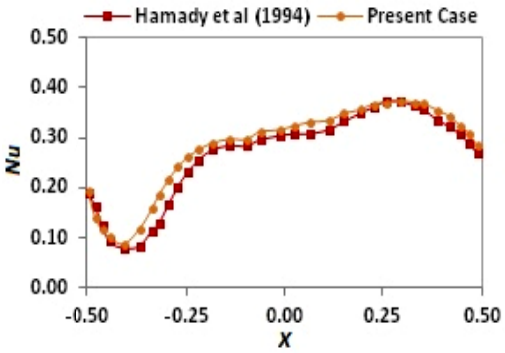

Fig. 5. Comprasion of computed dimensionless temperature along dimensiomless length for $Pr = 0.71, Ra = 1.1 \times 10^5\ and\ \Omega = 15\ rpm$.

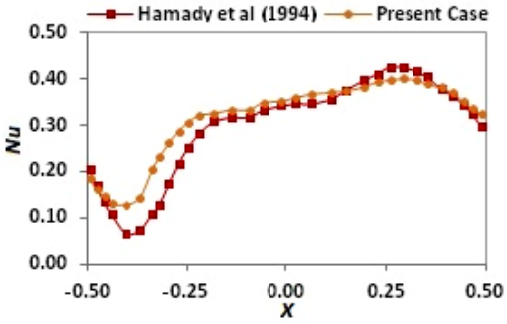

Fig .6. Comprasion of computed dimensionless temperature along dimensiomless length for$Pr = 0.71, Ra = 1.1 \times 10^5$ and $\Omega = 15\ rpm$.

Close agreement is obtained when compared with results of Hamady *et al*. (1994), who used the same governing equations and this gives confidence to the present simulation results.

4.2 Effect of Rotation on Flow and Temperature Fields

Fig. 7 (a) to Fig 10(a) represents the streamline and Fig. 7 (b) to Fig. 10 (b) shows isotherm counters for different rotational speed. The first column in these figures represents the90^o position of the enclosure, where the hot isothermal wall occupy relatively the left vertical position, the second column for 180^o positionwhere the hot isothermal wall occupy relatively the bottom horizontal position, the third column for270^o position where the hot isothermal wall occupy the relatively right vertical position and the last column for 360^o positionwhere the hot isothermal wall occupy relatively the top horizontal position of the enclosure.

For a fixed $Pr = 0.71$ and $Ra = 1.1 \times 10^5$and at $\Omega = 10\ rpm$, the thermal buoyancy is the dominating force compared to smaller magnitude of Coriolis forces due to the fact that the magnitude of the Taylor number is smaller when compared to the magnitude of Rayleigh number. As Coriolis force is a function of Taylor number and the thermal buoyancy is a function of Rayleigh number, Fig. 7(a) shows multi cellular roll pattern of stream function. The isotherms show thin boundary layer near isothermal walls with stable stratification of the core as evident from Fig. 7(b). At$\Omega = 15\ rpm$, the stream function [Fig. 8(a)] again shows formation of multiple rolls of slightly larger magnitude compared to the previous case. The isotherms in Fig. 8 (b) depict beginning of unstable stratification in the core signifying increase in convective motion in the core of the enclosure. The Coriolis forces are stronger near the walls but still their magnitude is quite small compared to the thermal buoyancy. Stable stratification of the core disruption takes place by opposing interaction of thermal and Coriolis forces which results in decrease of heat transfer, as the magnitude of the Taylor number and Rayleigh number is of same order. Further increase in rotation corresponding to $\Omega = 20\ rpm$ and$\Omega = 25\ rpm$, itresults in drastic change in the pattern formation of stream functions rolls as evident in Fig. 9 (a) and 10 (a). These figures show formation of counter rotating rolls towards the isothermal wall of the enclosure. These rolls are primarily formed due to the action of Coriolis forces on the fluid which offsets the eye of the streamline from the centre of the enclosure, as the magnitude of the Taylor number is larger when compared to the magnitude of Rayleigh number. Isotherms in Fig. 9 (a) and10 (b) shows generation of spiral shaped structure in the core of the enclosure which leads to strong unstable stratification of the core. Coriolis forces are more dominant force from centre of hot wall towards the cold wall which leads to the formation of spiral shaped isotherms.

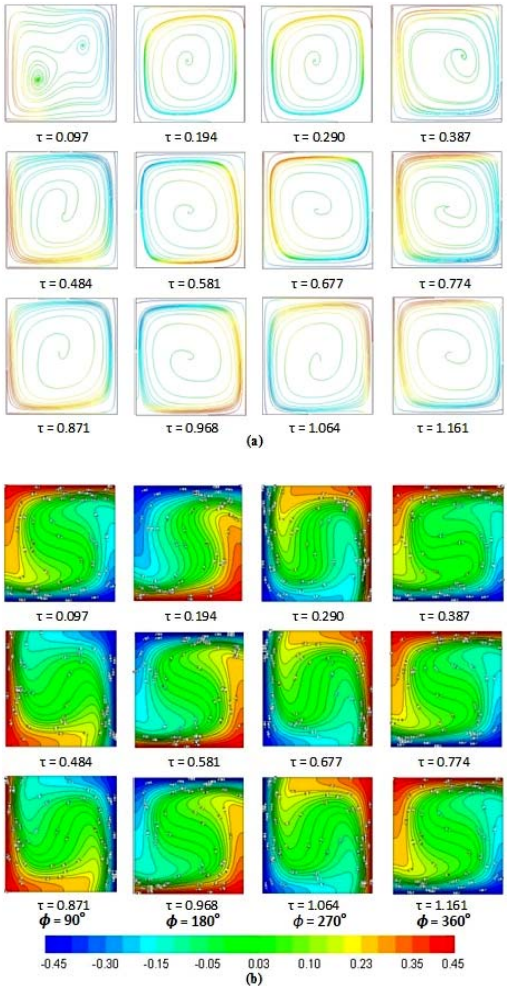

Fig. 7. (a) Streamline contours and (b) Isotherm contours for $Pr = 0.71, Ra = 1.1 \times 10^5$ and $\Omega = 10\ rpm$.

4.3 Effect of Rotations to Heat Transfer

For low rotation cases with $\Omega = 10\ rpm$and $\Omega = 15\ rpm$, thermal buoyancy force causes no local peaks in Nu and the flow consists of clockwise circulation. The clockwise circulation is enlarged and tends to cover the other circulation. It can be seen that with low rotation, the swing of Nu is suppressed by the thermal buoyancy which is evident from Fig. 11. With the increase in rotation speed to $\Omega = 20\ rpm$and $\Omega = 25\ rpm$,thermal

buoyancy force causes two or more local peaks in Nu and the flow consists of clockwise circulation, counter clockwise circulation and transition stages between them. The possible source of almost cyclic rise and fall of Nu is due to alternate domination of thermal buoyancy and Coriolis forces. Corresponding to the three local peaks, there are three inflexion points and the angle at the inflexion points are shown in Table 1.Fig. 11 shows unsteady and almost cyclic heat transfer at the walls. The minima correspond to the time interval when thermal buoyancy is dominant while the maxima correspond to the duration when Coriolis force is the dominating force. The effects due to rotation are summarized in Table 1.

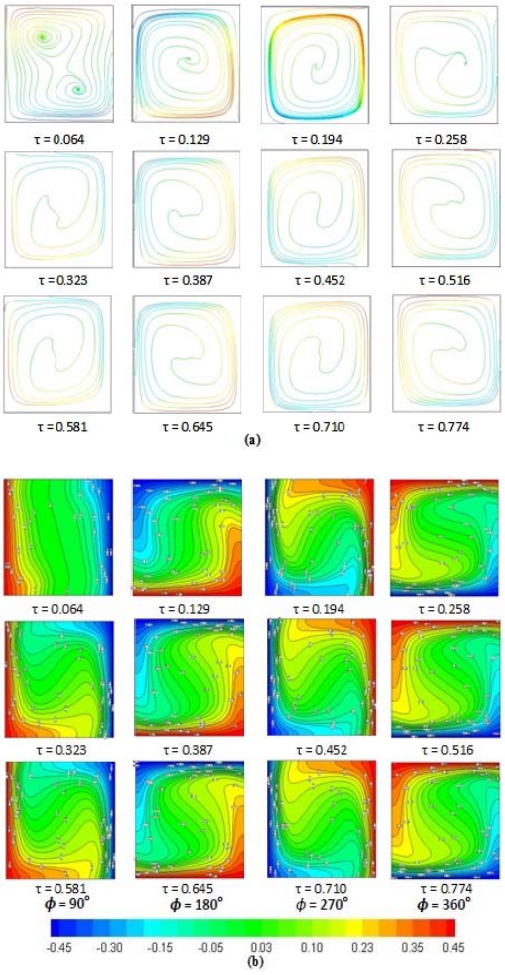

Fig .8. (a) Streamline contours and (b) Isotherm contours for $Pr = 0.71, Ra = 1.1 \times 10^5$ and $\Omega = 15\ rpm$

4.4 Effects of Rotations to Time and Space Averaged Heat Transfer

The transient behavior of the Nusselt number computed as a function of rotation is exhibited in Fig. 12. Initially, the heat transfer is sensitive to time and varies periodically with time. As time progresses this behavior disappears and the Nusselt number attains steadiness. At $\Omega = 10\ rpm$, the flow is dominated by the thermal buoyancy. At $\Omega = 5\ rpm$, there is disruption of heat transfer by opposing interaction of thermal and Coriolis force which results in decrease of $\overline{\overline{Nu}}$. For $\Omega = 20\ rpm$ and $25\ rpm$, the heat transfer is governed by Coriolis force and occurs not through the boundary layers but by the spiral shaped structure and hence there is rise of $\overline{\overline{Nu}}$. Thus rotation reduces heat transfer performance in the low rotation speed range and increases it in the relatively high speed ranges as shown in Fig. 13.

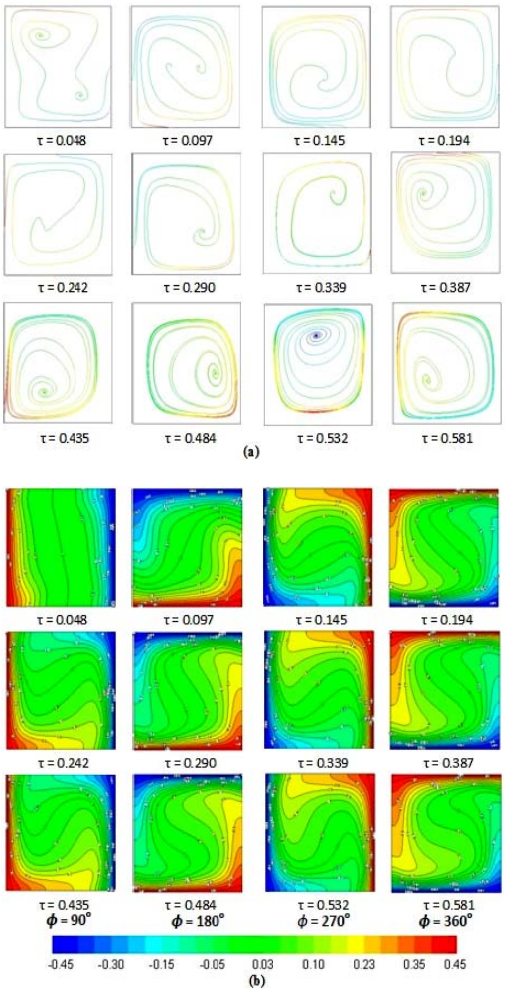

Fig. 9. (a) Streamline contours and (b) Isotherm contours for $Pr = 0.71, Ra = 1.1 \times 10^5$ and $\Omega = 20\ rpm$.

5. CONCLUSION

The following conclusions can be drawn from the present studies

1. For $\Omega = 10\ rpm$ and $\Omega = 15\ rpm$, the flow is dominated by the thermal buoyancy and suppresses the oscillation in $\overline{\overline{Nu}}$ and heat transfer is by thermal buoyancy effect.
2. For $\Omega = 15\ rpm$, there is disruption of heat transfer by opposing interaction of thermal and rotational buoyancy which results in decrease of heat transfer.
3. For $\Omega = 20\ rpm$ and $\Omega = 25\ rpm$ the angular location of the local maximum and minimum heat transfer are sensitive to rotational speeds.

Table 1 Effect of rotation ($Pr = 0.71,\ Ra = 1.1 \times 10^5$)

Ta	No of peaks Nu	$\overline{Nu}_{max}$	$\overline{Nu}_{min}$	$\frac{\Delta\overline{Nu}}{(\overline{Nu}_{max} - \overline{Nu}_{min})}$	ϕ_1	ϕ_2	ϕ_3
5.2×10^4	0	4.139	4.095	0.044	$\approx 30^o$	-	-
1.2×10^5	0	3.904	3.881	0.023	$\approx 0^o$	-	-
2.1×10^5	3	4.05	3.73	0.32	$\approx 60^o$	$\approx 180^o$	$\approx 300^o$
3.3×10^5	3	4.609	3.736	1.233	$\approx 90^o$	$\approx 210^o$	$\approx 330^o$

4. The local maximum and minimum points tends to move to higher angles when the enclosure is rotated at higher rotational speed.
5. At high rotational speed corresponding to $\Omega = 20\ rpm$and $\Omega = 25\ rpm$,there is alternate domination of Coriolis and thermal buoyancy forces and results in almost periodic variation of Nusselt number with time. The minima correspond to the time interval when thermal buoyancy is dominant while the maxima correspond to the duration when Coriolis force is the dominating force.
6. At high rotational speeds ($\Omega = 20\ rpm$and $\Omega = 25\ rpm$), there is significant increase in Nusselt number which is primarily due to domination of Coriolis forces and rotational buoyancy effect.

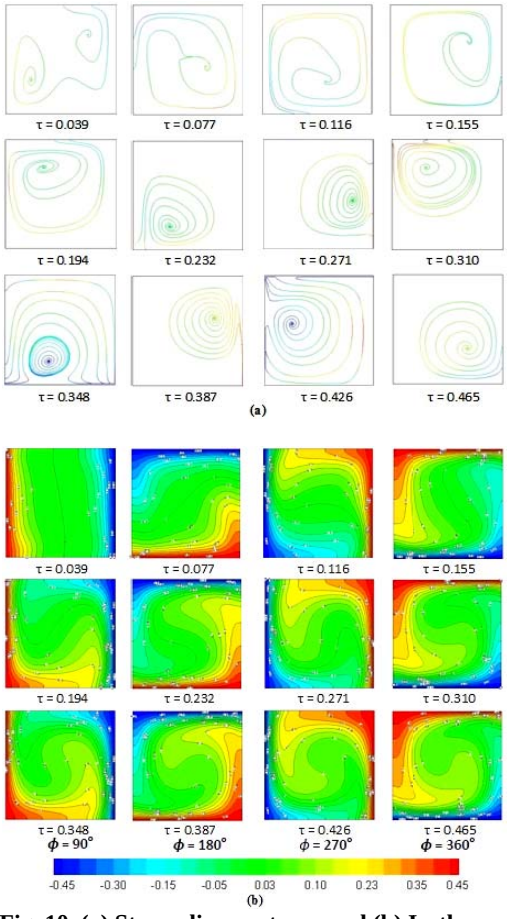

Fig. 10. (a) Streamline contours and (b) Isotherm contours for $Pr = 0.71, Ra = 1.1 \times 10^5$ and $\Omega = 25\ rpm$.

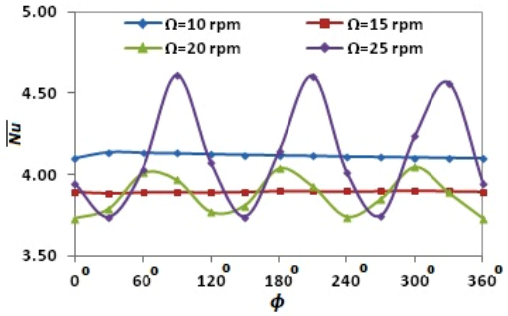

Fig. 11. Variation of Nusselt number with angular position of enclosure for $Pr = 0.71, Ra = 1.1 \times 10^5$.

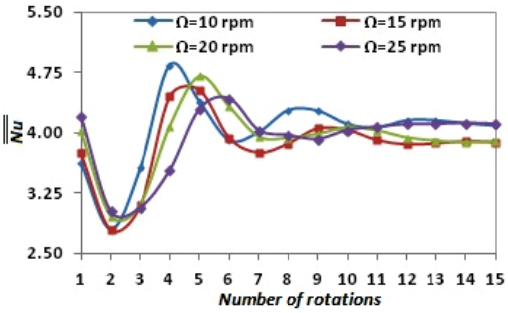

Fig. 12. Variation of time averaged Nusselt number with rotation for $Pr = 0.71$, $Ra = 1.1 \times 10^5$.

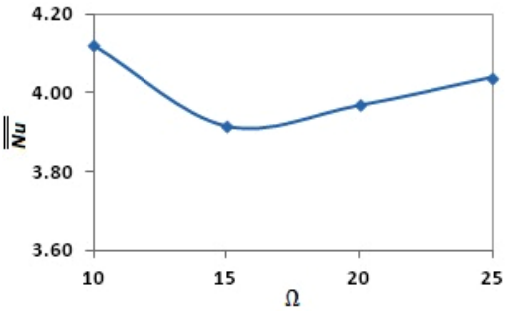

Fig. 13. Variation of time averaged Nusselt number with rotation ($Pr = 0.71$, $Ra = 1.1 \times 10^5$).

REFERENCES

Baig, M. F. and A. Masood (2001). Natural convection in a two-dimensional differentially heated square enclosure undergoing rotation. *Numerical Heat Transfer Part* A 40, 181–202.

Baig, M. F. and M. Zunaid (2006). Numerical simulation of liquid metals in differentially

heated enclosure undergoing orthogonal rotation. *International Journal of Heat and Mass Transfer* 49, 3500–3513.

Bobco, R. P. (1981). Free convection in enclosures exposed to compressive heating, Heat Transfer Therm. Control: Progr. *Astronaut. Aeronaut*. 78, 487–515.

BoubnovB.M., G.S. Golitsyn,(1995), *Convection in Rotating Fluids*. Kluwer Academic Publishers.

Buhler. K. and H. Oertel (1982). Thermal cellular convection in rotating rectangular boxes. *J. Fluid Mech*. 114, 261– 282.

Hamady, F. J., J. R. Lloyd, K. T. Yang and H. Q. Yang (1994). A study of natural convection in a rotating enclosure. *J. Heat Transfer* 116, 136–143.

Jin, L. F., S. K. W. Tou and C. P. Tso (2005). Effects of rotation on natural convection cooling from three rows of heat sources in a rectangular cavity. *International Journal of Heat and Mass Transfer* 48, 3982–3994.

Ker, Y. T. and T. F. Lin (1996). A combined numerical and experimental study of air convection in a differentially heated rotating cubic cavity. *International Journal of Heat and Mass Transfer* 39, 3193–3210.

Ker, Y. T. and T. F. Lin (1997). Time-averaged and reverse transition in oscillatory air convection in a differentially heated rotating cubic cavity. International Journal of Heat and *Mass Transfer* 40, 3335–3349

Lee, T. L. and T. F. Lin (1996). Transient three-dimensional convection of air in a differentially heated rotating cubic cavity. *International Journal of Heat and Mass Transfer* 39, 1243–1255.

Lin, Y. L., T. I. P. Shih, M. A. Stephens and M. K. Chyu (2001). A numerical study of flow and heat transfer in a smooth and ribbed U-Duct with and without rotation. *J. Heat Transfer* 123, 219–232.

Patankar, S. V. (1980). Numerical heat transfer and fluid flow. *Hemisphere Publishing Corporation.*

Rossby, H. T**. (**1969). A study of Benard convection with and without rotation**.** ***J.*** *Fluid Mech.* 36, 309-335**.**

Tso, C. P., L. F. Jin and S. K. W. Tou (2007). Numerical segregation of the effects of body forces in a rotating, differentially heated enclosure. *Numerical Heat Transfer Part A* 51, 85–107.

Vanyo, J. P. (1993). *Rotating Fluids in Engineering and Science*. Butterworth-Heinemann Press.

Yeh, L. T. (1995). Review of heat transfer technologies in electronic equipment. *J. Electron. Package*. 117, 333–339.